4506–4512 *Nucleic Acids Research, 1996, Vol. 24, No. 22*

Parallel and antiparallel A*A–T intramolecular triple helices

C. Dagneaux, H. Gousset, A. K. Shchyolkina[1], M. Ouali, R. Letellier, J. Liquier, V. L. Florentiev[1] and E. Taillandier*

Laboratoire CSSB - URA CNRS 1430, UFR de Santé-Médecine-Biologie-Humaine, Université Paris XIII, 74 Rue Marcel Cachin, 93017 Bobigny, France and [1]Engelhardt Institute of Molecular Biology RASc, Vavilova St 32, 117984 Moscow, Russian Federation

Received July 26, 1996; Revised and Accepted October 1, 1996

ABSTRACT

Intramolecular triple helices have been obtained by folding back twice oligonucleotides formed by decamers bound by non-nucleotide linkers: dA_{10}-linker-dA_{10}-linker-dT_{10} and dA_{10}-linker-dT_{10}-linker-dA_{10}. We have thus prepared two triple helices with forced third strand orientation, respectively antiparallel (apA*A–T) and parallel (pA*A–T) with respect to the adenosine strand of the Watson–Crick duplex. The existence of the triple helices has been shown by FTIR, UV and fluorescence spectroscopies. Similar melting temperatures have been obtained in very different oligomer concentration conditions (micromolar solutions for thermal denaturation classically followed by UV spectroscopy, milimolar solutions in the case of melting monitored by FTIR spectroscopy) showing that the triple helices are intramolecular. The stability of the parallel triplex is found to be slightly lower than that of the antiparallel (ΔT_m = 6°C). The sugar conformations determined by FTIR are different for both triplexes. Only South-type sugars are found in the antiparallel triplex whereas both South- and North-type sugars are detected in the parallel triplex. In this case, thymidine sugars have a South-type geometry, and the adenosine strand of the Watson–Crick duplex has North-type sugars. For the antiparallel triplex the experimental results and molecular modeling data are consistent with a reverse-Hoogsteen like third-strand base pairing and South-type sugar conformation. An energetically optimized model of the parallel A*A–T triple helix with a non-uniform distribution of sugar conformations is discussed.

INTRODUCTION

Many structures of triple helices have been reported, however little is known about the less stable A*A–T triplex (in this notation an '*' represents third strand binding and a '–' the Watson–Crick base pairing of the target duplex). It has been proposed that the formation of rA*rA–rU and rA*dA–dT intermolecular triplexes depended on the rA third strand length (1–2). Formation of the dA*dA–dT triplex in high salt conditions has been recently detected by CD spectroscopy (3). However no data concerning third strand orientation or conformations in A*A–T triplexes have been published. It appears that the A*A–T triplexes cannot be easily obtained from separate oligonucleotides. Intramolecular triplexes formed by folding back twice on itself an appropriate DNA sequence have enhanced stability when compared to triplexes obtained by the association of three separate DNA strands. Such systems composed by three oligonucleotide segments covalently bound either by two nucleotide loops (4–9) or by non-nucleotide linkers (10–13) have been successfully used for spectroscopic studies of triplexes other than A*A–T. The order of the segments and the direction of the coupling strictly determines the relative orientation of the strands in the formed triplex, and this strategy allows one to obtain triplexes with a third strand parallel or antiparallel to the identical strand of the Watson–Crick duplex (14–17).

In the present work, we have studied both parallel and antiparallel intramolecular triplexes containing only A*A–T base triplets using UV, fluorescence and FTIR spectroscopies. Oligomers dA_{10}-linker-dA_{10}-linker-dT_{10} and dA_{10}-linker-dT_{10}-linker-dA_{10} in which the three decamers are bound by two non-nucleotide linkers have been stabilized in presence of Mn^{2+} counterions respectively into the apA*A–T and the pA*A–T triplexes (ap = antiparallel; p = parallel) (Fig. 1). FTIR spectroscopy has proved to be well suited for the study of triple helical geometries in solution and characterization of sugar conformations (17–21). An additional advantage of non-nucleotide linkers for FTIR studies is that their vibrational spectrum does not present significant absorption bands in the spectral region used to characterize triplex formation.

In the pur*pur–pyr triplexes containing GA sequences, the third strand is generally oriented antiparallel (8,18,22–28). Triple helices containing both G*G–C and A*A–T base triplets with antiparallel third strand orientation have only South-type sugars (18). The apA*A–T structure studied in the present work is

* To whom correspondence should be addressed. Tel: +33 148387690; Fax: +33 148377443

This paper is dedicated to the memory of R. Letellier deceased at the age of 35

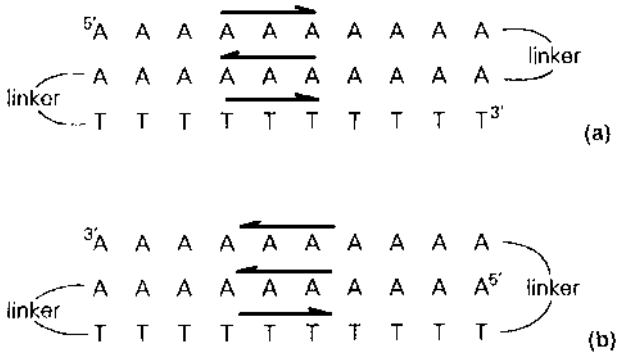

Figure 1. Intramolecular triple helices. (**a**) apA∗A–T triplex.; (**b**) pA∗A–T triplex.

similar to those of pur∗pur–pyr triplexes containing A∗A–T and G∗G–C base triplets, with only South-type sugars and reverse Hoogsteen base pairing.

Three stranded structures with parallel homologous strands have been considered as putative intermediates in genetic recombination. Different mechanisms have been proposed for the RecA mediated formation of joint molecules (29–33). The three stranded intermediate formed is a structure wherein the departing strand in the major groove is held in close association with the nascent heteroduplex. However the stereochemistries of the base triplets are not yet known. A base pairing scheme model has been proposed in which the base in the major groove is paired with both bases of the Watson–Crick duplex (34); dG∗dG–dC base triplets with parallel orientation have recently been observed by X-ray diffraction at the junction of two Watson–Crick duplexes packed in the crystal structure (35). FTIR studies performed on the dG∗dG–dC triple helix had shown a parallel third strand orientation and both North- and South-types sugars (North-type sugars have been assigned to the dG strand of the Watson–Crick duplex) (21). In the present work for the parallel pA∗A–T triplex, South- and North- type sugars have been found and the North-type sugars belong to the adenine strand of the Watson–Crick duplex. Molecular modeling shows that the energetically optimized structure for the parallel pA∗A–T triplex including this non-uniform sugar distribution is compatible with H-bond formation between third-strand adenine and both adenine and thymine bases of the targeted duplex.

MATERIALS AND METHODS

Sample preparation

Oligonucleotides dA_{10}-linker-dA_{10}-linker-dT_{10} and dA_{10}-linker-dT_{10}-linker-dA_{10} (Fig. 1), in which the linker is -pO(CH_2CH_2O)$_3$p, were purchased from Genset Paris, France. They were purified by HPLC and excess salt removed by elution on a G10 column. Stock solutions (80 µM strand) were heated at 80°C for 3 min. To obtain the antiparallel triplex dA_{10}-linker-dA_{10}-linker-dT_{10} samples were then directly stored at 4°C while to obtain the parallel triplex dA_{10}-linker-dT_{10}-linker-dA_{10} samples were slowly (12 h) cooled down to 4°C. For UV thermal denaturation experiments oligonucleotide concentration was 2.5 µM strand in 0.1 M $MnCl_2$. For fluorescence polarization measurements performed at 10°C, oligonucleotide concentration did not exceed 0.5 µM strand in 10 mM $MnCl_2$ and propidium iodide concentration was 0.15 µM. For FTIR spectroscopy the same samples were concentrated in the cold room to 3 mM strand. The final manganese content was 0.25 Mn^{2+} ion per base for the apA∗A–T triplex and 1 Mn^{2+} ion per base for the pA∗A–T triplex. Deuteration experiments were performed by evaporating sample solutions to dryness under nitrogen and then redissolving oligomers in the same volume of D_2O.

Vibrational spectroscopy

FTIR spectra were recorded using a Perkin Elmer 2000 Fourier transform spectrophotometer. Usually 15 scans were accumulated. Solution spectra were obtained in ZnSe cells. Temperature of the sample was controlled and monitored between 5°C and 60°C using a Specac temperature controller. FTIR data were treated with the Galaxy Grams program. This treatment includes spectral normalization using the phosphate symmetric stretching vibration at 1086 cm^{-1} as internal standard.

UV spectroscopy and fluorescence polarization measurements

Thermal denaturation curves were recorded at 260 nm with a Kontron Uvikon 941 spectrophotometer equipped with computer controlled thermostated cuvette holders. Temperature was varied at a constant heating rate of 6°C/h. Cell path lengths were 1 cm.

Measurements of fluorescence polarization of the dA_{10}-linker-dT_{10}-linker-dA_{10} oligonucleotide having an intercalated propidium iodide probe were performed at 10°C with a FluoroMax spectrofluorometer equipped with the Model 1935B polarization accessory (SPEX). Excitation and emission wavelengths were 520 nm and 610 nm, respectively. The excitation slit was 4 mm, the emission slit was 6 mm. The value of polarization was computed as : $P = (I_{vv}–GI_{vh})/(I_{vv}+GI_{vh})$ where G was the grating factor (I_{hv}/I_{hh}) and intensities I_{vv}, I_{hv} were the vertical and I_{vh}, I_{hh} the horizontal components of fluorescence, the first subscript indicating the position of the excitation polarizer (36). Averaged experimental errors were about 5%.

Molecular modeling

Conformational energy minimizations were performed with the JUMNA VII computer program developed by R. Lavery *et al.* (Junction Minimisation of Nucleic Acid) which has been successfully used for a large variety of nucleic acid structures (37). Starting geometries have been built by introducing into theoretical models the FTIR experimental data concerning sugar conformations. For the apA∗A–T triple helix (Fig. 2a), we have considered two initial structures which differ by the value of the glycosidic torsion angle (*syn* or *anti*) of third-strand nucleosides, as both geometries were *a priori* compatible with South-type sugar geometries and the proposed base pairing scheme.

For the pA∗A–T triple helix as the FTIR spectra showed the presence of both North- and South-type sugars, models have been constructed including North-type sugars either in the adenine strand of the Watson–Crick duplex or in the third strand. We have considered in our simulations the two different base pairing schemes previously proposed for parallel triplexes (34,38) (respectively Figs 2b and c). The pA∗A–T structures which have the lowest calculated energies have been compared with the experimental results.

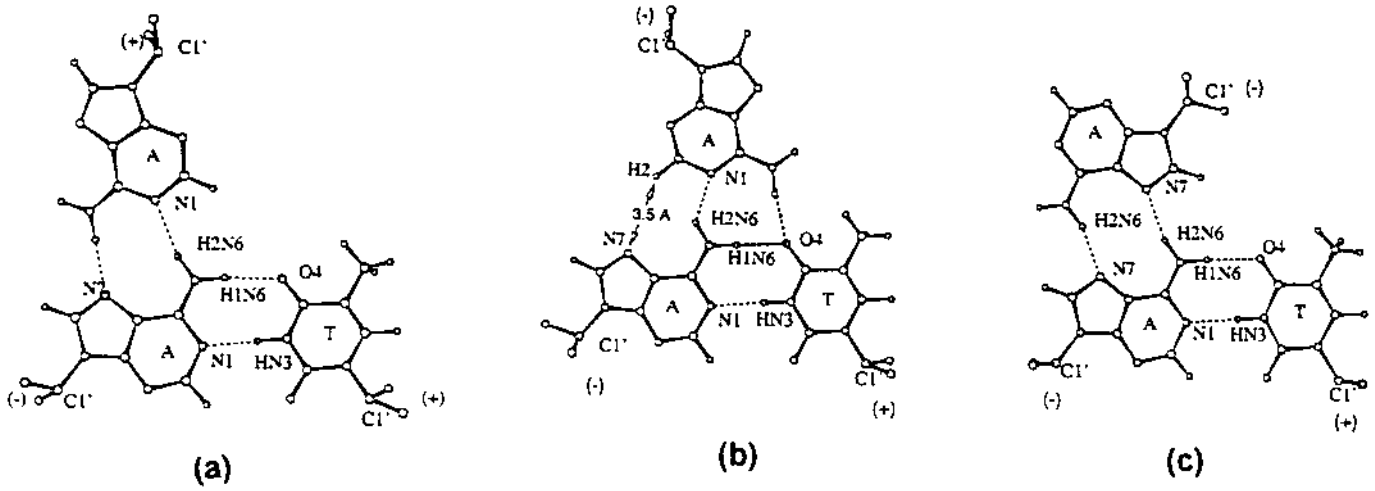

Figure 2. A∗A–T base triplet hydrogen bonding schemes. The plus and the minus indicate the relative strand polarity. (**a**) Reverse Hoogsteen type. (**b**) Type 1 from ref. (34). (**c**) Type 2 from ref. (38).

RESULTS

UV and fluorescence spectroscopies

The melting curve obtained for the dA_{10}-linker-dA_{10}-linker-dT_{10} oligonucleotide is presented in Figure 3a (open squares). The denaturation profile is clearly biphasic as shown by the derivative plot (inset). The first transition occurs at 24°C and is classically assigned to third strand separation of the apA∗A–T triple helix while the second transition at 57°C reflects the duplex melting.

The UV melting curve for the dA_{10}-linker-dT_{10}-linker-dA_{10} oligonucleotide is presented in Figure 3a (solid circles) and the corresponding derivative plot in the inset. It is also biphasic, third-strand separation occurs at 19°C while disruption of the Watson–Crick duplex is observed at 59°C. This shows that the parallel pA∗A–T triple helix has been formed. Parallel third strand orientation had previously been observed only for G∗G–C triplexes (21). When both G∗G–C and A∗A–T triples coexist the most stable orientation is antiparallel. To confirm the formation of this non-classical pA∗A–T parallel triple helix we have used fluorescence spectroscopy. The computed value of polarization P, which depends on the hydrodynamic volume of the structure (see Materials and Methods), is for the dA_{10}-linker-dT_{10}-linker-dA_{10} oligonucleotide (pA∗A–T) equal to 0.084. For the control triplex formed by a dT_{10}-linker-dT_{10}-linker-dA_{10} oligonucleotide (classical parallel pT∗A–T triple helix) the P value is 0.088. For the double-helical hairpin dT_{10}-linker-dA_{10}, in the same experimental conditions, the measured value was 0.058. In the case of dA_{10}-linker-dT_{10}-linker-dA_{10} oligomer (pA∗A–T), as linkers used are flexible hinges, binding of the third strand to the double-stranded part of the molecule leads to a P value close to that of the control triplex. The absence of triple helical structure would lead to a lower P value close to that of a control duplex or hairpin of same length (11,15). These results also show that the pA∗A–T triplex is formed.

Infrared spectroscopy: evidence of apA∗A–T and pA∗A–T triplex formation

The 1750 cm^{-1}–1550 cm^{-1} spectral domain contains absorption bands assigned to base in-plane double bond stretching vibrations. These absorption bands are sensitive to stacking and to hydrogen bond formation between bases in double (39–41) and triple helical structures (17,19,20).

The FTIR spectra of the apA∗A–T oligomer at 15°C and of the pA∗A–T oligomer at 10°C are presented respectively in Figure 4a and c (solid line). Absorption peaks are assigned by comparison with the spectrum of double stranded dA_{12}-dT_{12} (Fig. 4b) (17). Bands located at 1696 cm^{-1}, 1662 cm^{-1} and 1641 cm^{-1} are classically assigned mainly to C2=O2, C4=O4 and C=C double bond stretching vibrations of thymine bases involved in Watson–Crick base pairing. For thymines in single stranded oligomers the same vibrational modes are observed at 1692 cm^{-1}, 1663 cm^{-1} and 1632 cm^{-1}. The 1625 cm^{-1} absorption band is assigned to an adenine ring vibration involving C=C and C=N stretching motions coupled to an ND_2 scissoring vibration.

The relative intensity of this adenine vibration (taking the intensity of the 1086 cm^{-1} absorption band of the phophate groups as an internal standard) increases with temperature and has been used as a probe to follow the melting of the triple helices (Fig. 3b). In good agreement with the melting curves obtained using UV spectroscopy (Fig. 3a), biphasic melting profiles have been observed. The midpoint of the first transition is found at 23°C for the apA∗A–T triplex and at 16°C for the pA∗A–T triplex. As expected for unimolecular structures, denaturation of the triplex is not concentration dependent (3 mM oligomer for the FTIR profile and 2.5 µM for the UV profile). During this first transition no modifications are observed concerning the thymidine absorptions which shows that the duplex remains formed (Fig. 4a,c dash-dotted spectra). At higher temperatures the FTIR spectra show present thymidine absorption bands located at the positions of free thymidines (1692 cm^{-1} and 1662 cm^{-1}, while the 1641 cm^{-1} band is no longer observed) (Fig. 4a,c dotted spectra, recorded at 60°C). The second transition corresponds thus to duplex melting.

The pA∗A–T intramolecular triple helix is found slightly less stable than the apA∗A–T triple helix (ΔT_m = –5°C measured by UV or –7°C measured by FTIR). For intermolecular pur∗pur–pyr triple helices containing only G∗G–C base triplets the parallel orientation was more stable (actually it was the only one observed) (21,35). Introduction of A∗A–T base triplets favors the

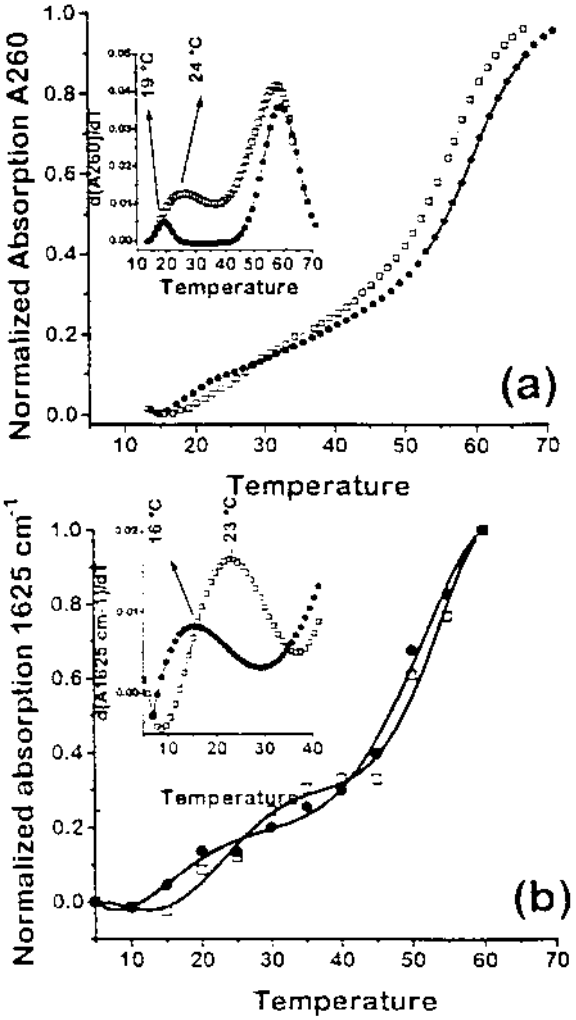

Figure 3. (**a**) UV melting curves of pA∗A–T triplex (solid circles) and apA∗A–T triplex (open squares). Inset: corresponding derivative curves dA_{220}/dT. (**b**) FTIR melting curves of pA∗A–T triplex (solid circles) and apA∗A–T triplex (open squares). Inset: corresponding derivative curves $dA_{1625cm-1}/dT$.

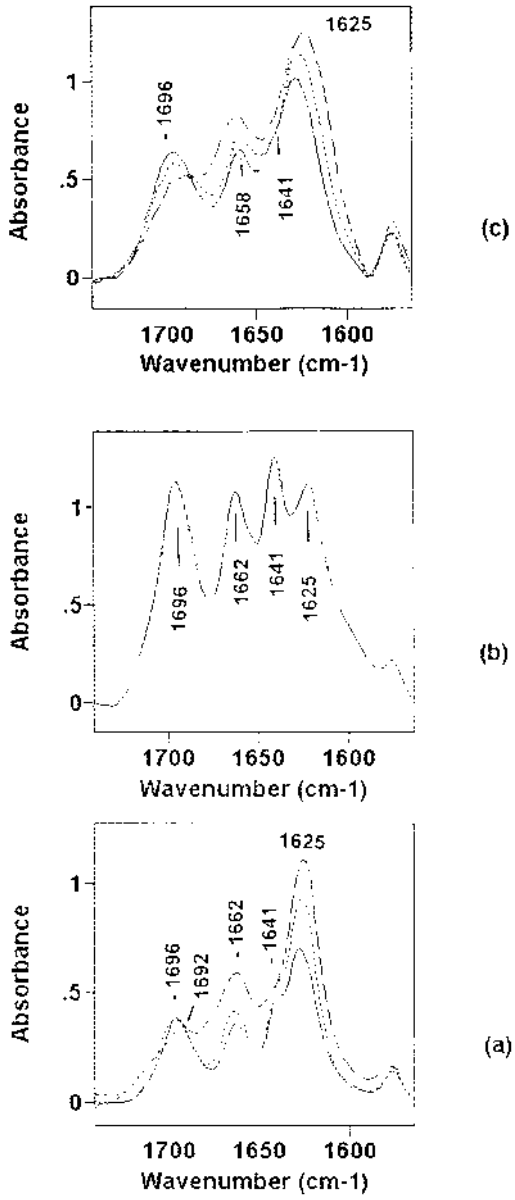

Figure 4. FTIR spectra in the base double bond stretching vibration region, recorded in D_2O solution of : (**a**) dA_{10}-linker-dA_{10}-linker-dT_{10} at 15°C (—) (apA∗A–T triplex), 35°C (·–·–·) (duplex with dA_{10} dangling end) and 60°C (-----). (**b**) dA_{12}-dT_{12} duplex. (**c**) dA_{10}-linker-dT_{10}-linker-dA_{10} at 10°C (—) (pA∗A–T triplex), 35°C (·–·–·) (duplex with dA_{10} dangling end) and 60°C (-----).

antiparallel orientation (8,22–28). This is in agreement with the present result for sequences containing only A∗A–T base triplets, in which the antiparallel third strand orientation is more stable than the parallel one.

A slight difference between the FTIR spectra of the pA∗A–T and apA∗A–T triple helices in this spectral region concerns the absorption mainly assigned to the C4=O4 thymine stretching vibration. This mode is observed at 1662 cm^{-1} in the apA∗A–T spectrum (Fig. 4a solid line) as in the A–T duplex spectrum (Fig. 4c) but at 1658 cm^{-1} in the pA∗A–T spectrum (Fig. 4c solid line) suggesting a different implication of the C4=O4 group in the third strand binding.

Sugar conformations in the apA∗A–T and the pA∗A–T triplexes

Sugar conformation marker bands in triple helical structures are found in the 900 cm^{-1}–750 cm^{-1} spectral region (39–41). The North-type sugar conformation is characterized by an absorption band observed around 865 cm^{-1}, whereas the South-type sugar conformation is reflected by an absorption band observed around 840 cm^{-1}. In the apA∗A–T triplex only South-type sugars are detected as shown by the absorption band at 842 cm^{-1} (Fig. 5d). In the pA∗A–T triplex spectrum recorded at 5°C, South-type (absorption band at 842 cm^{-1}) and North-type sugars (absorption band at 869 cm^{-1}) are observed (Fig. 5a). The ratio of the relative intensities of these two bands indicates that one-third of the sugars are in N-type conformation (one strand in the pA∗A–T triplex).

The strand containing the N-type sugars belongs to the Watson–Crick duplex as shown by comparing spectra presented

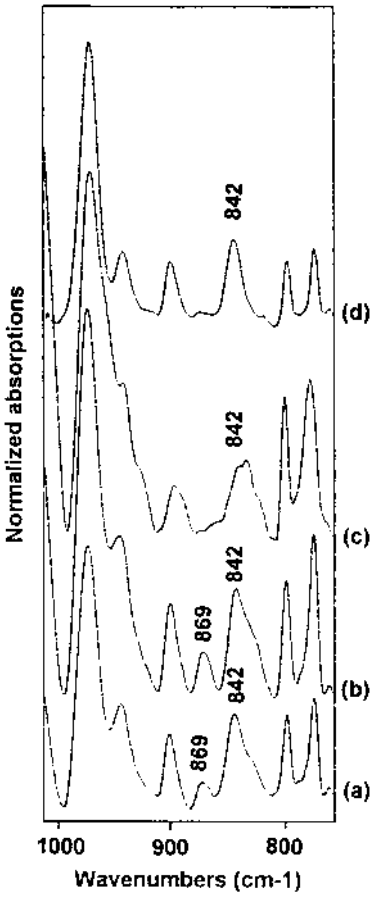

Figure 5. FTIR spectra in the sugar vibration region, recorded in D_2O solution of : (**a**) dA_{10}-linker-dT_{10}-linker-dA_{10} at 5°C (pA∗A–T triplex). (**b**) dA_{10}-linker-dT_{10}-linker-dA_{10} at 30°C. (**c**) dA_{10}-linker-dT_{10}-linker-dA_{10} at 55°C. (**d**) dA_{10}-linker-dA_{10}-linker-dT_{10} at 15°C (apA∗A–T triplex).

in Figure 5a,b and c. When the temperature is increased, separation of the third strand occurs first. On spectrum 5b recorded at 30°C, corresponding to the hairpin duplex with a dangling dA_{10} end, we still observe the North-type sugar contribution. When the temperature is further increased melting of the duplex takes place and no more North-type sugars are detected (spectrum Fig. 5c). Thus the North-type sugars in the pA∗A–T triplex belong to the hairpin duplex. Moreover a thymidine vibration band, detected at 1281 cm^{-1} in the pA∗A–T triplex spectrum indicates that thymidines have South-type sugars (42,43) (spectrum not shown). This allows us to assign the North-type sugars in the pA∗A–T triplex to the adenosines of the hairpin duplex.

Molecular modeling

Energy minimization calculations performed on the apA∗A–T triple helix show that the stucture with reverse Hoogsteen like H-bonding scheme (22) (Fig. 2a) and South-type sugar conformation is energetically most favorable when the glycosidic torsion angles of third-strand nucleosides have an *anti* conformation. This result is in agreement with correlations between the *anti* glycosidic torsion angle conformation of third-strand nucleosides and the reverse Hoogsteen like scheme previously found for pur∗pur–pyr triplexes with antiparallel orientation of the two purine strands (25,44). The *anti* base/sugar position has also been reported in the NMR study of an intramolecular triplex containing an antiparallel third strand with G–A and G–T steps (8).

Molecular mechanics calculations concerning the pA∗A–T triplex show that the model incorporating the suggestions proposed by the interpretation of infrared spectra, (the Watson–Crick adenosine strand with North-type sugars) and the base pairing scheme derived from the work of Zhurkin (34) (Fig. 2b) has the lowest conformational energy (Table 1, lines 1 and 2). Formation of H-bonds between the third strand and both bases of the duplex stabilizes the triple helix more efficiently than the model in which the third purine strand is H-bonded only to the Watson–Crick purine strand (38) (Fig. 2c). We can notice that in the most favourable base pairing scheme (Fig. 2b) the distance computed between the H2 site of the third strand adenine and the N7 site of the duplex adenine is 3.5 Å which is larger than the usually considered distance for strong electrostatic interactions (below 3 Å) (45).

Table 1. Molecular mechanics total energy values (kcal/mol) of the pA∗A–T triplex

Third strand base-pairing	Starting geometry	Total energy	Refined structure
From ref (34)	S/anti	–644	S/anti
	N/anti		N/anti
	S/anti		S/anti
From ref (38)	S/anti	–525	S/anti
	N/anti		N/anti
	S/anti		S/anti
From ref (34)	S/anti	–562	S/anti
	S/anti		S/anti
	N/anti		N/anti
From ref (38)	S/anti	–599	S/anti
	S/anti		S/anti
	N/anti		N/anti

The columns describing the starting geometry and the calculated structure specify the sugar pucker and glycosidic torsion angle of the dT_{10} strand (top), the Watson–Crick dA_{10} strand (middle) and the third dA_{10} strand (bottom) S (South) and N (North) correspond respectively to the C2'-endo and C3'-endo families.
In the initial structures, adenosines with North-type sugars are considered in the Watson Crick duplex (a) and in the third strand (b).

The computation shows the importance of the location of the strand containing adenosines with North-type sugars. We have considered models in which the North-type sugars belong to the third strand. The presence of adenosines with North-type sugars is energetically more favorable in the Watson–Crick strand rather than in the third strand, which is in agreement with the experimentally observed conformation (Table 1, lines 1, 3 and 4). If the third strand has North-type sugars and the duplex only South-type ones, third-strand binding to the target duplex induces

a destabilization of the duplex in which the backbone torsion angles adopt unfavorable non-canonical values.

The optimized pA∗A–T triple helix has a twist and a rise values respectively around 33° and 3 Å as in B family form DNA. The Xdisp parameters show that the Watson–Crick bases are shifted by almost 3 Å from the DNA axis towards the minor groove. For this structure, third-strand nucleosides have an *anti* glycosidic torsion angle conformation and the sugar-backbone torsion angles have standard values. The base triads have a good planarity as shown by the low values of the Inc and Tip parameters characteristic of base inclinations (Table 2).

Table 2. Helical parameters and conformational angles of the pA∗A–T structure having the lowest energy, reflecting the planarity of the base triads

	Xdisp	Ydisp	Rise	Inc	Tip	Twist	
dT (WC)	–2.96	0.17	3.22	2.55	–3.23	33.31	
dA (WC)	–2.92	–0.11	3.22	4.05	–13.40	33.31	
dA (Third)	–0.74	1.74	3.22	–0.25	–5.44	33.31	
	χ	α	β	γ	δ	ε	ξ
dT (WC)	243.4	–65.0	–173.9	54.7	135.0	–172.7	–110.4
dA (WC)	207.6	–76.0	–176.3	64.4	83.0	–161.0	–65.0
dA (Third)	254.3	–64.5	175.0	56.5	147.0	–168.9	–127.3

The parameters Xdisp (translation on the local dyad axis pointing toward the major groove), Ydisp (translation on the long axis oriented along the base-pair axis), Inc, and Tip (rotation parameters around respectively the same axis) give the position of the base in each strand with respect to a reference point defined as the intersection where the helical axis would cut the base plane in a standard B-conformation.Twist, rise and conformation angles refer to the usual definitions (49). WC, Watson-Crick strands; Third, third strand.

DISCUSSION

Evidence for formation of apA∗A–T and pA∗A–T triple helices has been shown by UV, fluorescence and FTIR spectroscopies, using oligonucleotides able to fold back twice on themselves and in presence of Mn^{2+} counterions.

A reverse Hoogsteen third strand binding and South-type sugars characterize the apA∗A–T triplex. An identical base pairing scheme and sugar geometry were earlier found for the apT∗A–T triple helix. This intramolecular triplex with forced antiparallel third strand orientation has been prepared by folding back twice on itself the dT_{10}-dA_{10}-dT_{10} oligomer. When the third thymidine strand was reversed from parallel (classical T∗A–T triple helix) to antiparallel then the base pairing scheme changed from Hoogsteen to reverse Hoogsteen. The sugar geometry in the apT∗A–T triple helix was also South-type (17). The existence of only South-type sugars in the apA∗A–T triplex is in agreement with earlier studies of triple helical structures containing simultaneously A∗A–T and G∗G–C base triplets with antiparallel third-strand orientation, in which only South-type sugars have been detected by NMR (8,9) and FTIR (18).

The parallel third strand orientation which was proposed using FTIR data in the case of a pur∗pur–pyr triple helix containing only G∗G–C base triplets (21) has recently been confirmed by an X-ray crystal diffraction study (35). The same distribution of sugar conformations between the three strands is found here for the pA∗A–T intramolecular triple helix as in the pG∗G–C intermolecular triple helix previously studied (North-type sugars for the purine duplex strand). The best energy minimized model of the pA∗A–T triple helix incorporating this new conformational constraint (non-uniform sugar geometry distribution) is obtained with a third strand base pairing scheme similar to that proposed by Zhurkin *et al.* (34). The base located in the major groove is hydrogen bound to both bases of the Watson–Crick duplex.

The computed helical parameters (twist = 33°, rise = 3.2 Å) show that in the pA∗A–T triple helix the duplex remains in the family of non-extended structures (for which these parameters are 20° and 5.1 Å) with base triplets essentially perpendicular to the DNA axis, but nevertheless deviates from a classical B form double helix in particular by the important displacement of the Watson–Crick base pairs towards the minor groove (Xdisp around 3 Å). Such deviation allows formation of the triple stranded structure without stretching of the helical structure.

The interest in parallel DNA triplexes has been recently stimulated by the discovery of their possible role in homologous genetic recombination. Three DNA strands can be brought into interaction within the RecA nucleoprotein filament, forming an extended three stranded complex which could serve as intermediate in homologous recombination (29,33,34,44,46). Such an extended structure reflects electron microscopy results demonstrating the lengthening and unwinding of the nucleic acid helix in presence of RecA (47). In the recombinant three stranded complex models the rise of the helix has been increased to 5.1 Å and all sugars adopt a North-type conformation (34). We have recently observed by FTIR North-type sugars in a parallel three stranded complex formed on a sequence containing all four bases in presence of RecA (48). It will be interesting to compare the pA∗A–T triplex structure and the three stranded AAT complex formed in the presence of RecA protein.

ACKNOWLEDGEMENTS

We thank the IDRIS supercomputer center (Institut du Développement des Ressources en Informatique Scientifique, CNRS, Orsay, France) for allocation of CRAY C98 computer time.

REFERENCES

1 Broitman,S.L., Im,D.D. and Fresco,J.R. (1987) *Proc. Natl. Acad. Sci. USA*, **84**, 5120–5124.
2 Letai,A.G., Palladino,M.A., Fromm,E., Rizzo,V. and Fresco,J.R. (1988) *Biochemistry*, **27**, 9108–9112.
3 Howard,F.B., Miles,H.T. and Ross,P.D. (1995) *Biochemistry*, **34**, 7135–7144.
4 Häner,R. and Dervan,P.B. (1990) *Biochemistry*, **29**, 9761–9765.
5 Radhakrishnan,I., De los Santos,C. and Patel,J.D. (1991) *J. Mol. Biol.*, **221**, 1403–1418.
6 Macaya,R.F., Schultze,P. and Feigon,J. (1992) *J. Am. Chem. Soc.*, **114**, 781–783.
7 Wang,E., Malek,S. and Feigon,J. (1992) *Biochemistry*, **31**, 4838–4846.
8 Radhakrishnan,I., De los Santos,C. and Patel,D.J. (1993) *J. Mol. Biol.*, **234**, 188–197.
9 Radhakrishnan,I.and Patel,D.J. (1993) *Current Biology-Structure*, **1**, 135–152.
10 Durand,M., Peloille,S., Thuong,N.T. and Maurizot,J.C. (1992) *Biochemistry*, **31**, 9197–9204.
11 Shchyolkina,A.K., Timofeev,E.N., Borisova,O.F., Il'cheva,I.A., Minyat,E.E., Khomyakova,E.B. and Florentiev,V.L. (1994) *FEBS Lett.* **339**, 113–118.
12 Bornet,O., Lancelot,G., Chanteloup,L., Thuong,N.T. and Beau,J.M. (1994) *J. Biomol. NMR*, **4**, 575–580.
13 Bornet,O. and Lancelot,G. (1995) *J. Biomol. Struct. Dyn.*, **12**, 803–814.

14 Shchyolkina,A.K., Lysov,Yu.P., Il'cheva,I.A., Chernyi,A.A., Golova,Yu.B., Chernov,B.K., Gottick,B.P. and Florentiev,V.L. (1989) *FEBS Letters*, **244**, 39–42.
15 Borisova,O.F., Golova,Yu.P., Gottikh,B.P., Zibrov,A.S., Il'cheva,I.A., Lysov,Yu.,P., Mamayeva,O.K., Chernov,B.K., Chernyi,A.A., Shchyolkina,A.K. and Florentiev,V.L. (1991) *J. Biomol. Struct. Dyn.*, **8**, 1187–1210.
16 Radhakrishnan,I. and Patel, D.J. (1994) *Biochemistry*, **33**, 11405–11416.
17 Dagneaux,C., Liquier,J and Taillandier,E. (1995) *Biochemistry*, **34**, 14815–14818.
18 Porumb,H., Dagneaux,C., Letellier,R., Malvy,C. and Taillandier,E. (1994) *Gene*, **149**, 101–107.
19 Liquier,J., Coffinier,P., Firon,M. and Taillandier,E. (1991) *J. Biomol. Struct. Dyn.*, **9**, 437–445.
20 Akhebat,A., Dagneaux,C., Liquier,J. and Taillandier,E. (1992) *J. Biomol. Struct. Dyn.*, **10**, 577–587.
21 Ouali,M., Letellier,R., Sun,J-S., Akhebat,A., Adnet,F., Liquier,J. and Taillandier,E. (1993) *J. Am. Chem. Soc.*, **115**, 4264–4270.
22 Beal,P.A. and Dervan,P.B. (1991) *Science*, **251**, 1360–1363.
23 Havre,P.A., Gunther,E.J., Gasparro,F.P. and Glazer,P.M. (1993) *Proc. Natl. Acad. Sci. USA*, **90**, 7879–7883.
24 Pilch,D.S., Levenson,C. and Shafer,R.H. (1991) *Biochemistry*, **30**, 6081–6087.
25 Washbrook,E. and Fox,K.R. (1994) *Nucleic Acids Res.*, **22**, 3977–3982.
26 Malkov,V.A., Voloshin,O.N., Soyfer,V.N. and Frank-Kamenetskii,M.D. (1993) *Nucleic Acids Res.*, **21**, 585–591.
27 Best,G.C. and Dervan,P.B. (1995) *J. Am. Chem. Soc.*, **117**, 1187–1193.
28 Ouali,M., Letellier,R. and Taillandier,E. (1996) *J. Mol. Struct.*, **377**, 57–74.
29 Rao,B.J. Dutreix,M. and Radding,C.M. (1991) *Proc. Natl. Acad. Sci USA*, **88**, 2984–2988.
30 Rao,B.J. and Radding,C.M. (1994) *Proc. Natl. Acad. Sci USA*, **91**, 6161–6165.
31 Hsieh,P., Camerini-Otero,C.S. and Camerini-Otero,R.D. (1990) *Genes Dev.*, **4**, 1951–1963.
32 Hsieh,P., Camerini-Otero,C.S. and Camerini-Otero,R.D. (1992) *Proc. Natl. Acad. Sci. USA*, **89**, 6492–6496.
33 Baliga, M., Singleton,J.W. and Dervan, P.B. (1995) *Proc. Natl. Acad. Sci. USA*, **92**, 10393–10397.
34 Zhurkin,V.B., Raghunathan,G., Ulyanov,N.B., Camerini-Otero,R.D. and Jernigan,R.L. (1994) *J. Mol. Biol.*, **239**, 181–200.
35 Van Meervelt,L., Vileghe,D., Dautant,A., Gallois,B., Précigoux,G. and Kennard,O. (1995) *Nature*, **374**, 742–744.
36 Minchenkova,L.E., Shchyolkina,A.K., Chernov,B.K. and Ivanov,V.I. (1986) *J. Biomol. Struct. Dyn.*, **4**, 463–475.
37 Lavery,R. (1988) In Olson,W.K., Sarma,M.H., Sarma,R.H. and Sundaralingam,M. (Eds.), *Structure and Expression Vol. 3 DNA Bending and Curvature*, Adenine Press, Guiderland New-York., pp. 191–171.
38 Piriou,J.M., Ketterlé,Ch., Gabarro-Arpa,J., Cognet,J.A.H. and Le Bret,M. (1994) *Biophysical Chemistry*, **50**, 319–343.
39 Tsuboï,M. (1969) In Brame,E.G.Jr. (Ed.), *Applied Spectroscopy Reviews*, M. Dekker, New-York, vol. 3, pp. 45–90.
40 Cao,A., Liquier,J. and Taillandier,E. (1995) In Schrader,B. (Ed.), *Infrared and Raman Spectroscopy of Biomolecules: Methods and Applications*, Weinheim Pub. Co., New York, pp. 344–372.
41 Liquier,J., Taillandier,E. (1996) In Mantsch,H.H and Chapman,D. (Eds) *Infrared Spectroscopy of Biomolecules*, Wiley-Liss Pub. Co., New York.
42 Adam,S., Liquier,J., Taboury,J.A. and Taillandier,E. (1986) *Biochemistry*, **21**, 3180–3225.
43 Liquier,J., Akhebat,A., Taillandier,E., Ceolin,F., Huynh Dinh,T. and Igolen,J. (1991) *Spectrochimica Acta*, **47A**, 177–186.
44 Laugthon,C.A and Neidle,S. (1992) *Nucleic Acids Res.*, **16**, 6535–6541.
45 Taylor,R. and Kennard,O. (1982) *J. Am. Chem. Soc.*, **104**, 5063–5070.
46 Kim,M.G., Zhurkin,V.B., Camerini-Otero,C.S. and Camerini-Otero,R.D. (1993) In Sarma,R.H & Sarma,M.H. (Eds), *Structural Biology : The State of The Art*, Adenine Press New York, vol. 2, pp. 67–74.
47 Stasiak,A., DiCapua,E. and Koller,Th. (1981) *J. Mol. Biol.*, **151,** 557–564.
48 Dagneaux,C., Porumb,H., Liquier,J., Takahashi,M. and Taillandier,E. (1995) *J. Biomol. Struct. Dyn.*, **13**, 465–470.
49 IUPAC-IUB Joint Commission on Biochemical Nomenclature. Abbreviations and symbols for the description of conformations of polynucleotide chains. (1983) *Eur. J. Biochem.*, **131,** 9–15.